EVALUATION OF WHEAT GROWTH MONITORING METHODS BASED ON HYPERSPECTRAL DATA OF LATER GRAIN FILLING AND HEADING STAGES IN WESTERN AUSTRALIA

T. Nakanishi [a] *, Y. Imai [a], T. Morita [a], Y. Akamatsu [a], S. Odagawa [b], T. Takeda [c] and O. Kashimura [c]

[a] Kokusai Kogyo Co., Ltd. 2-24-1 Harumi-cho, Fuchu-shi, Tokyo, 183-0057, Japan - (taira_nakanishi, yasuteru_imai, taichi_morita, yukio_akamatsu)@kk-grp.jp
[b] Asia Air Survey Co., Ltd. 1-2-2 Manpukuji, Asao-ku, Kawasaki-shi, Kanagawa, 215-0004, Japan - sh.odagawa@ajiko.co.jp
[c] Japan Space Systems. 3-5-8 Shibakoen, Minato-ku, Tokyo, 105-0011, Japan - (takeda-tomomi, kashimura-osamu)@jspacesystems.or.jp

Commission VIII/6, Agriculture, Ecosystems and Bio-Diversity

KEY WORDS: Hyperspectral imaging, Remote monitoring, Agricultural products, Moisture, LAI

ABSTRACT:

This study estimated the wheat yield, quality, and growth conditions using hyperspectral data of the later grain filling and heading stages. The study area is located in the suburbs of Mullewa, Western Australia. Various data used included spectral reflectance of wheat measured from the ground and those measured using airborne sensors, wheat growth conditions data, such as LAI, SPAD values, and wheat height, and sample analysis data, including biomass, grain nitrogen content rate, leaf nitrogen content rate, and ash content, of the later grain filling and heading stages. This study consisted of (1) selection of estimation items regarding the wheat yield, quality, and growth conditions by correlation analysis of sample data, (2) definition of estimate equations for selected items, (3) verification of estimation accuracy, and (4) development of estimation maps. As a result, head moisture, which is related to the wheat growth conditions, was well estimated using hyperspectral data of the later grain filling stage. At the same time, grain weight, which is related to the wheat yield, and grain nitrogen content rate and ash content, which are related to the wheat quality, were well estimated using hyperspectral data of the heading stage. This study implies that it is possible to visualize the wheat yield, quality, and growth conditions on a regional scale using hyperspectral data.

1. INTRODUCTION

Australia plays a key role to ensure food security of Japan. Approximately 90% of wheat consumed in Japan is imported from overseas countries. Among all countries, Australia is the thrid most important country because raw materials used to produce noodles in Japan are imported mostly from Australia. However, the Australian wheat production is vulnerable to natural disasters such as droughts. Therefore, it is desirable to develop the growth monitoring system to ensure the stable Australian wheat supply in the future.

Profitable agriculture requires efficient and precise estimation method for crop growth monitoring. Spaceborne sensors with a high wavelength resolution can improve the efficiency and precision of the estimation. The Ministry of Economy, Trade and Industry (METI) of Japan plays a leading role in the development of the satellite-borne hyperspectral sensor, HISUI (Hyper-spectral Imager SUIte), and researches on fundamental technology for hyperspectral data's applications in various fields such as energy, natural resources, agriculture, forestry, and the environment. In the field of agriculture, hyperspectral imaging is experimentally used to estimate the yield, quality, and growth of rice and wheat. Accordingly, we evaluated methods to estimate the wheat yield, quality, and growth conditions using ground-based and airborne hyperspectral data of the later grain filling and heading stages in Western Australia.

2. STUDY AREA

The study area is located in the suburbs of Mullewa, Western Australia (Figure 1). The area is approximately 480km² with mostly flat land features, and is mainly used for wheat, canola, and lupin fields which size is several square kilometers.

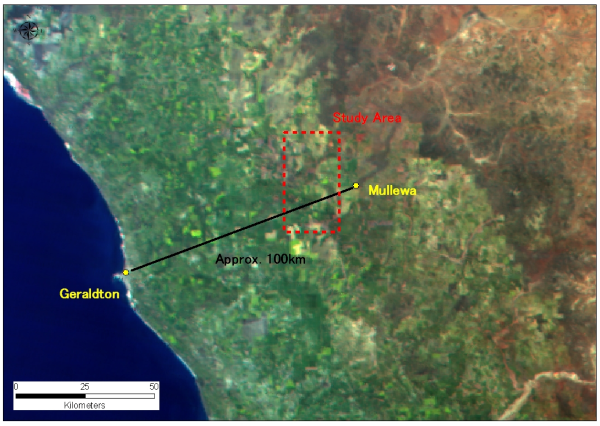

Figure 1: Study Area

3. DATA USED

The first field survey was conducted in the late October, which is around the same time as the later grain filling stage of wheat, of the year 2009 (Table 1). Ground-based hyperspectral data

---

* Corresponding author.

were acquired between October 14th and 16th using the FieldSpec Pro and FieldSpec Pro FR (ASD Inc., the U.S.), portable hyperspectral sensors, while airborne hyperspectral data were acquired in October 29th using the HyMap (HyVista Corporation, Austraria), an airborne hyperspectral sensor.

The second field survey was conducted between the late August and early September, which is around the same time as the heading stage of wheat, of the year 2010 (Table 1). Ground-based hyperspectral data were acquired between August 25th and September 2nd using the FieldSpec 3 FR and FieldSpec Pro FR, while airborne hyperspectral data were acquired in September 6th using the HyMap.

Table 1: Data Used for this Study and Observation Date

Data Type	Observation Date	
	First Survey	Second Survey
FieldSpec	2009/10/14-2009/10/16	2010/08/25-2010/09/02
HyMap	2009/10/29	2010/9/6
Growth Conditions Data	2009/10/13-2009/10/15	2010/08/24-2010/09/06, 2010/10/14-201010/19
Sample Analysis Data	2009/10/16-2009/10/20	2010/08/24-2010/09/06, 2010/10/14-2010/10/19

3.1 Specifications of Ground-based Hyperspectral Data

To acquire ground-based hyperspectral data and conduct plant sampling, the total 30 and 33 quadrats (10m by 10m) were installed for the later grain filling and heading stage observations respectively. In the field surveys, the reflectance spectra were measured at northwest, southwest, and southeast corners of each sample quadrat. To acquire typical spectral data, two sets of ridge, furrow, ridge and furrow were repeatedly measured from approximately 1m above a head of wheat (Figure 2). The measurement wavelength ranged from 350nm to 2,500nm, and the wavelength resolution was 1nm.

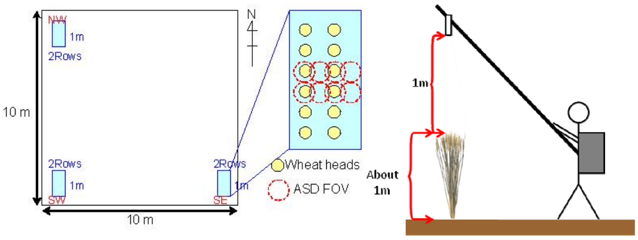

Figure 2: Overview of Quadrat (Left)
and Acquisition Method (Right)

3.2 Specifications of Airborne Hyperspectral Data

For the airborne surveys using the HyMap, the flight height was 2,250m, and the number of flight lines was nine. The observation wavelengths ranged from 440 to 2,480nm. The number of bands was 126, and the wavelength resolution was approximately 20nm. The view angle was 60 degrees, and the spatial resolution was about 4.2m.

3.3 Acquisition of Wheat Growth Conditions Data

For the later grain filling stage observation, the Leaf Area Index (LAI) and wheat height were measured at each sample point of the 30 quadrats around the same time as the ground-based reflectance spectra measurement. Wheat samples were also collected in the field. The number of wheat heads were counted, and the wet and dry wheat weights were also measured. After threshing, the wheat grain weight was measured, and 15 components, including the grain nitrogen content rate, were analyzed.

For the heading stage observation, the LAI, SPAD values, and wheat height were measured in the 33 quadrats around the same time as the ground-based reflectance spectra measurement. Wheat samples were also collected in the field. The number of wheat heads was counted, and wet and dry wheat weights were measured. After threshing, the wheat grain weight was measured, and 17 components, including the leaf nitrogen content rate, were analyzed. For the year 2010, wheat samples were collected again from October 14th to 19th, which is during the harvesting stage. The number of wheat heads, grain weight, and biomass were measured, and 17 components, including the grain nitrogen content rate, were analyzed.

4. METHODS

This study involved (1) estimation items selection, (2) estimation equation derivation, (3) estimation accuracy verification, and (4) estimation map development. Regarding the estimation equation derivation, the PLS regression was used for the heading stage observation only (Figure 3).

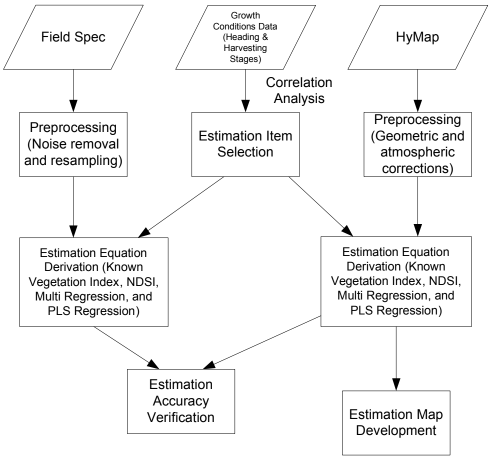

Figure 3: Workflow of this Study

4.1 Estimation Items Selection

The sample wheat data were analyzed to examine correlations between wheat features, and estimation items that are related to the wheat yield, quality, and growth conditions were determined. The sample wheat data of the heading stage were collected around the same time as ground-based and airborne hyperspectral data acquisition. The sample wheat data of the harvesting stage were also analyzed to examine correlations, and estimation items that are related to the wheat yield and quality were estimated.

4.2 Estimation Methods

For the later grain filling stage observation, (1) known vegetation index, (2) normalized differential spectral index (NDSI) (Inoue et al., 2008), and (3) multi regression analysis were examined. For the heading stage observation, (1) known vegetation index, (2) NDSI, (3) multi regression analysis, and (4) PLS regression analysis were examined. Using these estimation methods, correlations between the reflectance spectra measured using the FieldSpec and the HyMap, and the selected estimation items were examined. Finally, an estimation equation was derived from the analysis results.

4.3 Estimation Accuracy Verification

For estimation items that implied a relatively high degree of conformance, the estimated values and actual measured values were compared, and the estimation accuracy was verified.

4.4 Estimation Map Development

For estimation items that implied a relatively high degree of conformance, estimation maps that cover the entire study area were developed based on the HyMap hyperspectral data.

5. RESULTS AND DISCUSSION

5.1 Selection of Estimation Items

5.1.1 Later Grain Filling Stage

Table 2 shows correlation coefficients between the sample wheat data. For the grain weight, which is related to the wheat yield, an extremely high correlation between the dry stem weight and biomass (the total dry weight of head and stem) was determined (R: 0.9 or higher). The correlation between the grain weight and the number of heads was also determined (R: 0.76). For the grain nitrogen content rate, which is related to the wheat quality, a weak correlation with LAI was determined (R: 0.59). For the head moisture, which is related to the growth conditions, correlations with other estimation items were not determined. Biomass and LAI were also selected as estimation items, and the estimation methods using hyperspectral data were examined for these selected items (Figure 4).

Table 2: Correlations between Estimation Items for Later Grain Filling Stage

	LAI	The Number of Heads	Stem Dry Weight (g)	Total Biomass (g)	Grain Weight (g)	Height (cm)	Head Moisture (%)	Grain Nitrogen (%)	Grain Phosphorus (%)	Grain Potassium (%)
LAI										
The Number of Heads	0.68									
Stem Dry Weight (g)	**0.73**	**0.72**								
Total Biomass (g)	0.68	**0.76**	**0.96**							
Grain Weight (g)	0.54	**0.76**	**0.82**	**0.94**						
Height (cm)	0.47	0.36	0.64	0.51	0.36					
Head Moisture (%)	-0.46	-0.46	-0.39	-0.31	-0.24	-0.51				
Grain Nitrogen (%)	0.59	0.44	0.40	0.40	0.33	-0.01	-0.01			
Grain Phosphorus	0.44	0.42	0.23	0.30	0.32	-0.19	-0.31	0.58		
Grain Potassium (%)	0.28	0.12	0.06	0.05	-0.01	-0.29	-0.11	0.49	0.62	

▨	0.4 to 0.5
▨	0.5 to 0.6
▨	0.6 to 0.7
■	0.7 to 0.8
■	0.8 or higher

N=30

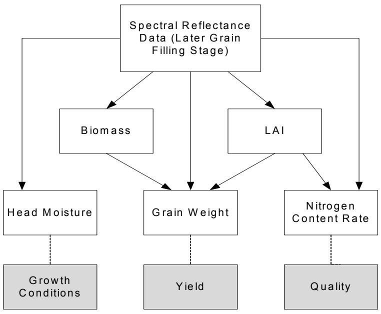

Figure 4: Estimation Items for Later Grain Filling Stage

5.1.2 Heading Stage

Table 3 shows correlation coefficients between the sample wheat data. For the grain weight, relatively high correlations with biomass of the heading stage and biomass of harvesting stage were determined (R: about 0.7). For the grain nitrogen content rate, a very high correlation with leaf nitrogen content rate was determined (R: 0.83), and correlations with LAI and SPAD values were also determined (R: about 0.7). For the ash content, which is related to the wheat quality, correlations with other estimation items were not determined. Biomass, LAI, SPAD values, and leaf nitrogen content rate were also selected as estimation items, and the estimation methods using hyperspectral data were examined for these selected items (Figure 5).

Table 3: Correlations between Estimation Items for Heading Stage

		Heading Stage						Harvesting Stage				
		LAI	SPAD	Culm Length (cm)	Biomass (g)	Moisture Content (%)	Leaf Nitrogen Content Rate (%)	The Number of Heads	Grain Weight (g)	Biomass (g)	Grain Nitrogen Content Rate (%)	Ash Content (%)
Heading Stage	LAI											
	SPAD	0.58										
	Culm Length (cm)	0.37	0.41									
	Biomass (g)	0.39	0.58	0.52								
	Moisture Content (%)	0.34	0.39	-0.24	0.26							
	Leaf Nitrogen Content Rate (%)	0.63	0.58	-0.12	0.19	0.51						
Harvesting Stage	The Number of Heads	0.51	0.44	0.05	0.56	0.49	**0.70**					
	Grain Weight (g)	0.10	0.30	0.50	0.69	0.02	-0.08	0.36				
	Biomass (g)	0.53	0.65	0.44	**0.81**	0.33	0.43	**0.79**	**0.74**			
	Grain Nitrogen Content Rate (%)	0.68	**0.72**	0.00	0.36	0.64	**0.83**	0.65	-0.08	0.49		
	Ash Content (%)	-0.26	-0.22	-0.40	-0.18	0.35	0.08	0.07	-0.40	-0.23	0.08	

▨	0.5～0.6
▨	0.6～0.7
■	0.7～0.8
■	0.8～

N=33

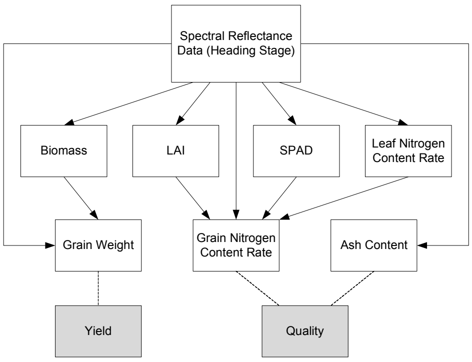

Figure 5: Estimation Items for Heading Stage

5.2 Examinations of the Estimation Methods

5.2.1 Later Grain Filling Stage

Table 4 shows estimation results of the selected estimation items using the three estimation methods. For the head moisture and LAI, the multi regression analysis using the FieldSpec and HyMap showed a relatively high determination coefficient (R^2: 0.6 or over). In the multi regression equation for the head moisture, the short wavelength infrared region (SWIR) was selected. However, the previous case study of rice indicated that the reflectance ratio of SWIR increases as the head moisture decreases (Shibayama and Akiyama, 1989). Therefore, it is possible that a similar situation will occur to the case of wheat. For the known vegetation index for the LAI, the cellulose absorption index (CAI) indicated a relatively high determination coefficient, and the wavelength band around 2,200nm was selected for the multi regression equation.

For the grain weight, nitrogen content rate, and biomass, all estimation methods showed a low determination coefficient. This situation implied that it is difficult to develop an estimation equation.

Table 4: Determination Coefficient
for Later Grain Filling Stage

Item	Methodology		FieldSpec		HyMap	
			R^2	Wavelength (nm)	R^2	Wavelength (nm)
Grain Weight (g)	Known Index	mNDVI	0.046	705, 750	0.099	705, 750
		CAI	0.104	2000, 2100, 2200	0.140	2000, 2100, 2200
		NDLI	0.143	1680, 1754	0.003	1680, 1754
	NDSI		0.399	1140, 1190	0.410	1480, 1500
	Multi Regression		0.380	1220, 1730	0.368	1200, 1430, 1720
Grain Nitrogen Content Rate (%)	Known Index	rbNDVI	0.042	445, 630	0.076	445, 630
		NDNI	0.043	1510, 1680	0.130	1510, 1680
	NDSI		0.445	1640, 1660	0.495	1460, 2130
	Multi Regression		0.501	1330, 1970	0.540	680, 1980
Head Moisture (%)	Known Index	NDWI	0.128	860, 1240	0.272	860, 1240
		WBI	0.631	900, 970	0.430	900, 970
	Depth of water absorption band		0.571	970	0.226	970
	NDSI		0.547	2010, 2020	0.624	1200, 1280
	Multi Regression		0.691	750, 1720, 2090	0.840	1720, 2090, 2270
Biomass (g)	Known Index	SR	0.237	665, 845	0.331	665, 845
		NDVI	0.248	665, 845	0.330	665, 845
		mNDVI	0.028	705, 750	0.151	705, 750
		SGR	0.023	500 … 599	0.035	500 … 599
		PRI	0.192	531, 570	0.094	531, 570
		RGR	0.002	500 … 599, 600 … 699	0.046	500 … 599, 600 … 699
		PI2	0.050	695, 760	0.186	695, 760
		CAI	0.155	2000, 2100, 2200	0.174	2000, 2100, 2200
		NDLI	0.230	1680, 1754	0.009	1680, 1754
	NDSI		0.512	1120, 1220	0.456	1140, 1450
	Multi Regression		0.545	620, 1770	0.592	1320, 1950
LAI	Known Index	SR	0.123	665, 845	0.347	665, 845
		NDVI	0.136	665, 845	0.354	665, 845
		mNDVI	0.008	705, 750	0.065	705, 750
		SGR	0.038	500 … 599	0.086	500 … 599
		PRI	0.479	531, 570	0.331	531, 570
		RGR	0.026	500 … 599, 600 … 699	0.084	500 … 599, 600 … 699
		PI2	0.001	695, 760	0.094	695, 760
		CAI	0.529	2000, 2100, 2200	0.509	2000, 2100, 2200
		NDLI	0.132	1680, 1754	0.000	1680, 1754
	NDSI		0.538	2130, 2160	0.583	1530, 1600
	Multi Regression		0.681	1480, 2080, 2270	0.859	680, 1470, 2280

■: Determination coefficient of 0.6 or higher

5.2.2 Heading Stage

Table 5 shows estimation results of the selected estimation items using the four estimation methods. The grain nitrogen content rate, SPAD values, and leaf nitrogen content rate indicated a high determination coefficient (R^2: 0.8 or over). The multi regression analysis was the most appropriate method for the grain nitrogen content rate, while the PLS regression was the most appropriate method for the SPAD values and leaf nitrogen content rate. The grain weight, ash content, biomass, and LAI also indicated a relatively high determination coefficient (R^2: 0.6 or over). The multi regression analysis was the most appropriate method for the ash content and LAI, while the multi regression analysis using the FieldSpec was the most appropriate method for the grain weight and biomass. For the HyMap, the PLS regression using the HyMap was the most appropriate method for the same estimation items.

Table 5: Determination Coefficient for Heading Stage

Item	Methodology		FieldSpec		HyMap	
			R^2	Wavelengh (nm)	R^2	Wavelength (nm)
Grain Weight (g)	Known Index	mNDVI	0.047	705, 750	0.024	705, 750
		CAI	0.252	2000, 2100, 2200	0.215	2000, 2100, 2200
		NDLI	0.075	1680, 1754	0.020	1680, 1754
	NDSI		0.433	780, 781	0.451	486, 1546
	Multi Regression		**0.489**	530, 1372, 2098, 2421	0.506	530, 721, 1206, 1573, 1726, 2100, 2277
	PLS Regression		0.456	All wavelengths	**0.661**	All wavelengths
Grain Nitrogen Content Rate (%)	Known Index	rbNDVI	0.349	445, 630		445, 630
		NDNI	0.471	1510, 1680	0.598	1510, 1680
	NDSI		0.715	742, 743	0.750	1206, 1331
	Multi Regression		**0.822**	363, 613, 769, 1460, 1776, 2028	**0.813**	707, 764, 1047, 1220, 2025, 2242
	PLS Regression		0.646	All wavelength	0.680	All wavelength
Ash Content (%)	NDSI		0.552	455, 460	0.563	894, 911
	Multi Regression		**0.689**	478, 721, 762, 1000, 1209, 2207	**0.697**	692, 764, 1047, 1330, 1676, 2360
	PLS Regression		0.611	All wavelength	0.625	All wavelength
Biomass (g)	Known Index	SR	0.317	665, 845	0.134	665, 845
		NDVI	0.372	665, 845	0.281	665, 845
		mNDVI	0.371	705, 750	0.267	705, 750
		SGR	0.151	500 … 599	0.075	500 … 599
		PRI	0.431	531, 570	0.335	531, 570
		RGR	0.390	500 … 599, 600 … 699	0.351	500 … 599, 600 … 699
		PI2	0.367	695, 760	0.273	695, 760
		CAI	0.498	2000, 2100, 2200	0.468	2000, 2100, 2200
		NDLI	0.335	1680, 1754	0.085	1680, 1754
	NDSI		0.593	1222, 1223	0.575	2171, 2260
	Multi Regression		**0.714**	712, 1055, 1209, 1550, 1728, 2102, 2273	0.621	721, 911, 1206, 1586, 1726, 2099, 2277
	PLS Regression		0.566	All wavelengths	**0.658**	All wavelengths
LAI	Known Index	SR	0.259	665, 845	0.357	665, 845
		NDVI	0.379	665, 845	0.377	665, 845
		mNDVI	0.378	705, 750	0.376	705, 750
		SGR	0.134	500 … 599	0.092	500 … 599
		PRI	0.361	531, 570	0.432	531, 570
		RGR	0.248	500 … 599, 600 … 699	0.363	500 … 599, 600 … 699
		PI2	0.399	695, 760	0.385	695, 760
		CAI	0.259	2000, 2100, 2200	0.364	2000, 2100, 2200
		NDLI	0.328	1680, 1754	0.405	1680, 1754
	NDSI		0.586	1188, 1216	0.644	2044, 2393
	Multi Regression		**0.640**	354, 478, 688, 2013, 2421	**0.728**	764, 911, 2045, 2409
	PLS Regression		0.432	All wavelength	0.634	All wavelength
SPAD	Known Index	SR	0.289	665, 845	0.230	665, 845
		NDVI	0.441	665, 845	0.344	665, 845
		mNDVI	0.446	705, 750	0.348	705, 750
		SGR	0.207	500 … 599	0.126	500 … 599
		PRI	0.480	531, 570	0.426	531, 570
		RGR	0.253	500 … 599, 600 … 699	0.286	500 … 599, 600 … 699
		PI2	0.455	695, 760	0.359	695, 760
		CAI	0.435	2000, 2100, 2200	0.459	2000, 2100, 2200
		NDLI	0.277	1680, 1754	0.164	1680, 1754
	NDSI		0.685	540, 542	0.575	530, 560
	Multi Regression		0.794	364, 699, 875, 1047, 1762, 2275	0.698	707, 911, 1047, 1206, 1477, 2277
	PLS Regression		**0.851**	All wavelengths	**0.852**	All wavelengths
Leaf Nitrogen Content Rate (%)	Known Index	rbNDVI	0.273	445, 630		445, 630
		NDNI	0.352	1510, 1680	0.477	1510, 1680
	NDSI		0.653	459, 468	0.627	736, 764
	Multi Regression		0.775	356, 635, 763, 1460, 1784, 2006, 2227, 2398	0.821	707, 764, 1047, 1220, 1663, 2360
	PLS Regression		**0.859**	All wavelengths	**0.933**	All wavelengths

■: Determination coefficient of 0.6 or higher

The accuracies of grain weight, grain nitrogen content rate, and ash content of the heading stage, and head moisture of the later grain filling stage showed a high degree of conformance, and their estimation accuracies were verified (Table 6).

Table 6: Determination Coefficient Analysis Results

Estimation Items		Heading Stage	Later Grain Filling Stage
Yield	Grain Weight	○(R^2=0.66)	×(R^2=0.31)
	Biomass	○(R^2=0.66)	△(R^2=0.59)
Quality	Grain Nitrogen Content Rate	◎(R^2=0.81)	△(R^2=0.54)
	Ash Content	○(R^2=0.70)	－
	Leaf Nitrogen Content Rate	◎(R^2=0.93)	－
	LAI	○(R^2=0.73)	◎(R^2=0.86)
	SPAD Value	◎(R^2=0.94)	－
Growth Conditions	Head Moisture	－	◎(R^2=0.84)

■: Time periods appropriate for estimation

5.3 Estimation Accuracy Verification

For the grain weight, grain nitrogen content rate, ash content, and head moisture, estimated values and actual measured values were compared. In order to verify influences of soil texture differences, comparison results were separately plotted based on soil color (Figure 6). For example, the head moisture in a red color soil area is usually low (approximately 10%), and the growth speed is generally high. The magnitude relation of quadrats was mostly replicated. At the same time, The grain weight, grain nitrogen content rate, and ash content indicated that the estimated values well corresponded to the actual measured values. The determination coefficients for these items were 0.66, 0.81, and 0.70 respectively. Indirect estimations through the biomass, LAI, and SPAD values showed a good degree of conformance. However, these indirect estimation results did not exceed direct estimation results. For the grain weight, grain nitrogen content rate, and ash content, relations with soil color were not observed.

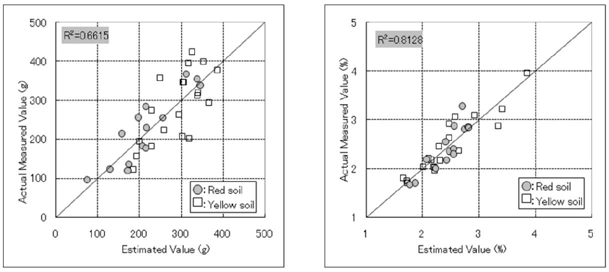

(a) Grain Weight (b) Grain Nitrogen Content Rate

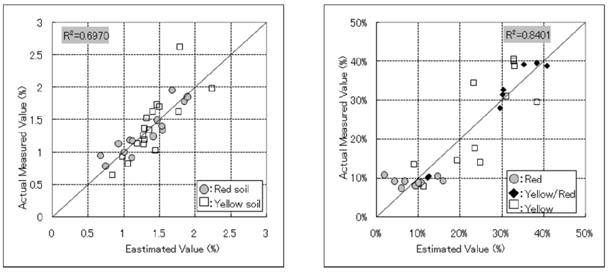

(c) Ash Content (d) Head Moisture

Figure 6: Comparison Results of Estimated and Actual Measured Values

5.4 Estimation Map Development

Estimation maps of the grain weight, grain nitrogen content rate, and ash content were developed by applying the developed estimation model to the entire HyMap data considering local conditions of the study area. In the same manner, an estimation map of the head moisture was also developed (Figure 7). The estimation map corresponded to the distribution pattern of soil color. The red color soil area indicated a low degree of head moisture, while the yellow color soil area showed a high degree of head moisture. To sum up, it is possible to visualize the wheat yield, quality, and growth conditions on a regional scale using the hyperspectral data of the heading and later grain filling stages.

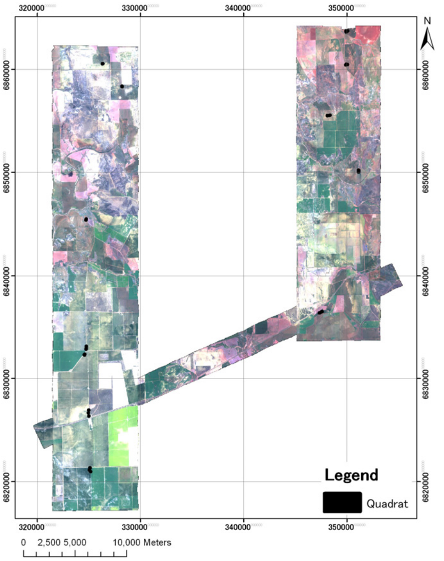

(a) HyMap Imagery of Heading Stage

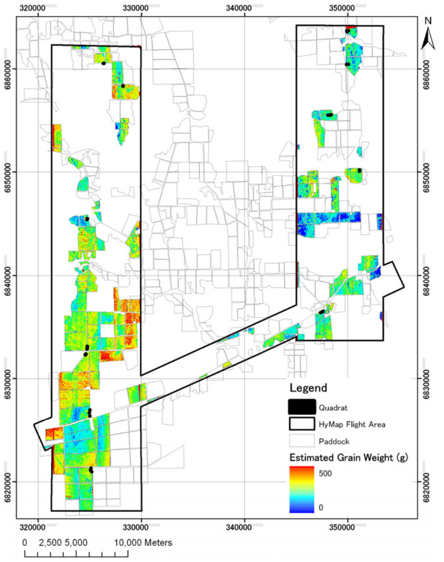

(b) Grain Weight

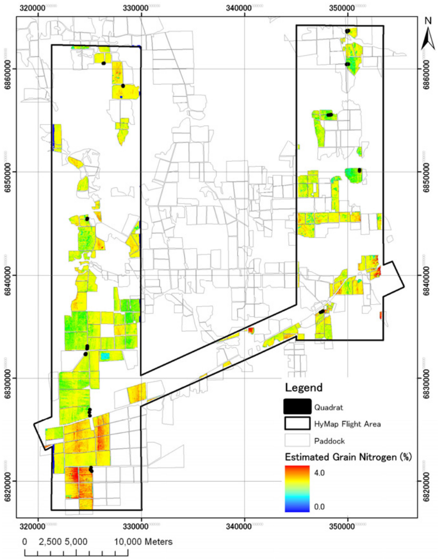

(c) Grain Nitrogen Content

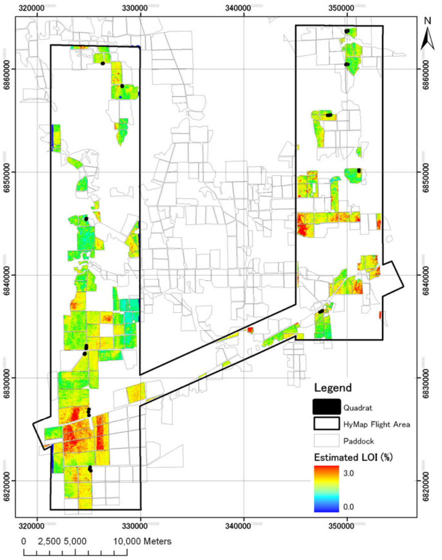

(d) Ash Content

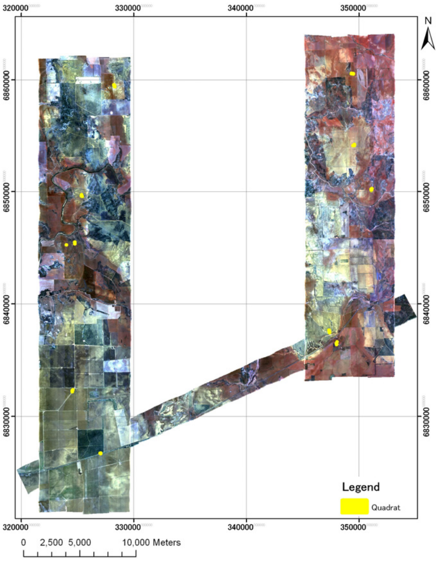

(e) HyMap Imagery of Later Grain Filling Stage

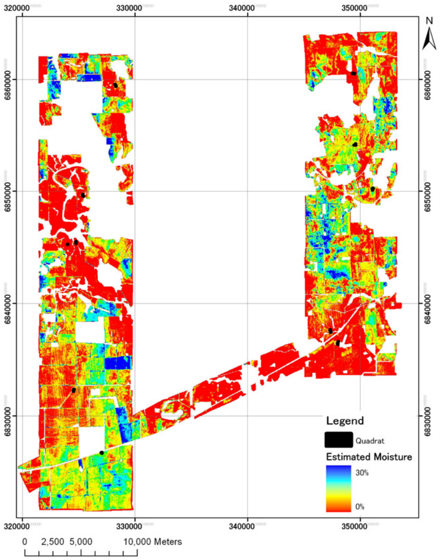

(f) Head Moisture

Figure 7: Estimation Maps based on HyMap Imagery

6. CONCLUSION

Estimation methods for the wheat yield, quality, and growth conditions were evaluated using both the ground-based and airborne hyperspectral data of the suburbs of Mullewa, Western Australia. This study revealed that the head moisture was well estimated by the multi regression analysis using the hyperspectral data of the later grain filling stage. This also indicated that the grain weight was well estimated by the PLS regression analysis, and the grain nitrogen content rate and ash content were well estimated by the multi regression analysis using the hyperspectral data of the heading stage. To sum up, this study achieved certain results of the development of the monitoring method for the wheat yield, quality, and growth conditions using hyperspectral data of the later grain filling and heading stages. For the future, the estimation accuracy will be improved by modifying the estimation methods. It is also possible that the estimation methods will be examined in different regions.

7. ACKNOWLEDGEMENT

This study was conducted as part of the project, 'The 2009 and 2010 Research and Development of the Fundamental Technology for Next-generation Satellite Utilizations,' of the former Earth Remote Sensing Data Analysis Center (ERSDAC).

We sincerely thank Dr. Tom Cudahy and Dr. Ian C Lau at the Commonwealth Scientific and Industrial Research Organization (CSIRO) and Mr. Buddy Wheaton and Dr. Daniel Carter at the Department of Agriculture and Food, Western Australia (DAFWA) for their help in the field study and airborne observations.

8. REFERENCES

Imai, Y., Morita, T., Akamatsu, Y., Odagawa, S., Takeda, T., and Kashimura, O., 2011. Evaluation of wheat growth monitoring methods based on hyperspectral data in western Australia. In: *IGARSS 2011: IEEE International Geoscience and Remote Sensing Symposium Proceedings*, pp. 3338-3341.

Inoue, Y., Peñuelas, P., Miyata, A., and Mano, M., 2008. Normalized difference spectral indices for estimating photosynthetic efficiency and capacity at a canopy scale derived from hyperspectral and CO2 flux measurements in rice. In: *Remote Sensing of Environment*, vol. 1112, pp. 156-172.

Shibayama, M. and Akiyama, T., 1989. Seasonal visible, near-infrared and mid-infrared spectra of rice canopies in relation to LAI and above-ground dry phytomass. In: *Remote Sensing of Environment*, vol. 27, pp. 119-127.